Electronic Supplementary Material (ESI) for Catalysis Science & Technology.
This journal is © The Royal Society of Chemistry 2021

Supporting Information

Tailoring the synergistic dual decoration of (Cu-Co) Transition Metal species in Fe-oxide/zeolite composite catalyst for the direct conversion of Syngas to Aromatics

Muhammad Asif Nawaz†, Maria Saif †, Minzhe Li, Guiyao Song, Wang Zihao and Dianhua Liu*

State Key Laboratory of Chemical Engineering, East China University of Science and Technology, Shanghai 200237, China

†These authors contributed equally to this work.

*Corresponding Author: dhliu@ecust.edu.cn

1. Catalyst Characterization

X-ray diffraction spectroscopy (XRD)

A Rigaku D/max2550V X-ray diffractometer was used to analyze the crystal morphology of the material, using Cu Kα (λ = 1.5406 Å) ray radiation source operated at 40 kV and 100 mA, with 0.02 °/s scanning rate.

Scanning electron microscope (SEM) & High-resolution transmission electron microscopy (HR-TEM)

Surface morphology and crystalline structure chemical composition of the catalyst were analyzed by Scanning electron microscopy (SEM, TESCAN MIRA3 XM) and Tecnai G2 20 S-Twin High-resolution transmission electron microscope (HR-TEM) at 200 kV. While performing scanning electron microscopy analysis, an X-ray energy spectrometer model of Aztec X-MAX50 was used to perform X-ray microanalysis on the sample to investigate the element composition of the catalyst surface.

N_2 adsorption-desorption

The surface area and pore size/volume of calcined catalyst was characterized by BET analysis with a nitrogen physical adsorption instrument of American company ASAP 2020-M. Inductively coupled plasma (ICP) was carried out on Agilent 5110 analyzer for the elemental composition of different metal oxides. First, degas under 200 °C vacuum conditions for 10 hours, and then obtain adsorption and desorption isotherms in liquid nitrogen atmosphere at -196 °C. The multi-point Brunauer-Emmett-Teller (BET) method is used to calculate the specific surface area (SBET) of the material according to Barrett -Joyner-Halenda (BJH) model fits the pore size distribution, and calculates the total pore volume (Vt) with the amount of N_2 adsorbed at a relative pressure of 0.985.

X-ray photoelectron spectroscopy (XPS)

XPS analysis was performed with ESCALAB 25 multifunctional photoelectron spectrometer. Test conditions: Monochromatic Hua Al target ray, the studio voltage is lower than 2×10-8 Torr (1 Torr=133.3 Pa). The standard electron binding energy of the C1s peak was 284.6 eV for charging correction for all the patterns, and the fitting program XPSPEAK4.1 was used for peak separation.

Temperature programmed Analysis (H_2-TPR, & CO/ CO_2-TPD)

All of the gases were introduced into a purification system in the temperature programmed process prior to sample cells, maintaining the gas (Ar for H_2 and He for CO/CO_2) flows at 50 ml/min with a temperature ramp of 10 °C/min, using Micrometrics AutoChem II 2920 analyzer, USA. Typically, 0.1g of catalyst was loaded into a quartz sample tube (10 mm i.d.) and a flow of 5 % H_2 in He was used as reduction gas. The effluent gas was analyzed by a thermal conductivity detector (TCD) to monitor the concentration variation of H_2. The catalyst was then reduced under H_2 with the temperature increasing from 50 to 800 °C.

Similarly, the catalyst sample was loaded into the sample cell and the temperature was kept at 150 °C with He flow for 60 min to remove the adsorbed species on the catalyst. First, the catalyst (0.1 g) was pretreated at 400 °C for 60 min in a flow of pure Ar of 60 mL min^{-1} and then cooled to 50 °C. After that, the catalyst was saturated in flowing CO_2 for 1 h with 30 mL min^{-1} and followed by flushing in Ar for 1 h to remove any physiosorbed molecules. Next, the CO/CO_2 desorption behaviors were recorded with the temperature increasing from 50-800 °C.

Electron paramagnetic resonance (EPR)

EPR spectra were recorded on a Bruker A300-10/12 spectrometer at 77 K.

Raman spectra

Raman spectra were obtained on a microscopic confocal Thermo Scientific DXR Raman spectrometer with a 532 nm excitation laser with 20 scans per spectrum and 1 cm^{-1} resolution.

Thermal weight loss analysis (TGA)

US TA SDT Q600 thermal analyzer was used to analyze the thermal weight loss behavior of the material. Under air or nitrogen atmosphere, maintaining a gas flow rate of (50 cm^3/min), heating to 800 °C at a heating rate of 10 °C /min, and obtaining a thermal weight loss curve to calculate the phase change and carbon deposition of spent catalyst samples.

Mössbauer effect spectroscopy (MES)

The Mössbauer spectra (MES) of the used samples were collected at room temperature (25 °C) on a Mössbauer spectrometer (Wissel, Germany) equipped with 57Co in a Pd matrix radioactive source moving in a constant acceleration mode. The spectra were collected over 512 channels in the mirror image format while operating the spectrometer in a symmetric constant acceleration mode and obtained the spectrum with a gas detector using least-square method to fit the spectra. The isomer shift, quadruple splitting and magnetic hyperfine field in the spectrum were used to identify certain iron phases. The spectral components were identified based on their isomer shift (IS), quadruple splitting (QS), and magnetic hyperfine field (Hhf).

1.1 Catalytic Evaluation

The feed gas with the molar ratio of 8:4:1 (H_2: CO: N_2), was premixed at 200 °C in a preheating box prior to the entrance of the fixed bed reactor configuration. Two thermocouples were mounted in the fixed bed to regulate the temperature of preheat chamber and reactor timely. The adiabatic condition (± 1 °C) in the catalyst bed was guaranteed through the axial temperature profile with a coated coaxial thermocouple in the center of the reactor, while correcting the mass flowmeter and thermocouple prior to the reaction in order to reduce errors.

Subsequently, 4g of physically mixed (in equal 2g mass ratio of metal catalyst and zeolite) catalysts were loaded into the isothermal zone of the reactor for the catalytic activity test. The composite catalyst was also mixed with quartz sand of equal mass to eliminate the influence of temperature gradient of a strong exothermic reaction and avoid excessive local temperature. The metal oxide catalyst was in-situ reduced before the experimental evaluation starts in flowing H_2 and N_2 (H_2:N_2=50:50 vol, GHSV=1500 h^{-1}) at 400 °C for 4 h. After the completion of reduction step, the temperature was cooled down to the reaction temperature and the reducing gas was switched to the reaction gas (CO+H_2) (containing 7% N_2) and subsequently introduced into the reactor by setting the process conditions as temperature 330-370 °C, GHSV 1000-3500 h^{-1}, pressure 2.0-5.0 MPa and H_2/CO ratio of 1/1 to 3/1. Before the start of the experiment, the leakage test was also performed by introducing nitrogen is into the reactor, and adjusting the pressure slightly greater than the reaction pressure.

After the reaction was stable, the gas phase product was subjected to a soap cell flow meter to calculate the outlet flow rate. Each experiment was done for 2-3 times and the average catalytic performances were collected after every 12 h, for which the gas phase product was analyzed by online gas chromatography using Agilent 7890B gas chromatograph. The Agilent 7890B gas chromatograph consists of two thermal conductivity detectors (TCD) and a hydrogen ion flame detector (FID) using N_2 as a reference gas for product analysis. Whereas, the liquid phase product was analyzed by PE Clarus 580 gas chromatograph categorizing as C_5^+ aliphatic and aromatic hydrocarbons. The particular calculation method of conversion and selectivity was calculated on the molar carbon basis and the detailed method is listed in supplementary material, while the calculated carbon balances were all higher than 90 %.

The reactor tube was cooled down before unloading the catalyst after the reduction and reaction under N_2 environment until room temperature (25 °C). After the catalyst was cooled down, it was subjected to passivation process under flowing 1% O_2 in N_2 at room temperature (25 °C) for 3 h for the purpose of specific reduced and spent catalysts characterization [1]. Due to the magnetic property of metal catalyst, the composite catalyst was unloaded and separated into metal catalyst and HZSM-5 by ultrasonic concussion and magnetism after the reaction, for the characterization respectively.

1.2 Product calculation method

The calculation formula of CO conversion rate and product carbon-based selectivity is as follows:

$$\chi_{CO} = \frac{n_{CO,\ in} - n_{CO,out}}{n_{CO,\ in}} \times 100\% \tag{3-1}$$

$$S_i = \frac{I \times n_i}{n_{CO,in} - n_{CO,out}} \times 100\% \tag{3-2}$$

In the formula (3-1), χ_{CO} represents the conversion rate of CO, and $n_{CO,in}$ and $n_{CO,out}$ respectively represent the molar amount of CO imported and exported Molar quantity; in formula (3-2), I represents the carbon number of reaction product i, and n_i represents the molar quantity of reaction product. All data in the experiment are the average of three repeated experiments.

2. Characterization and Experimental data

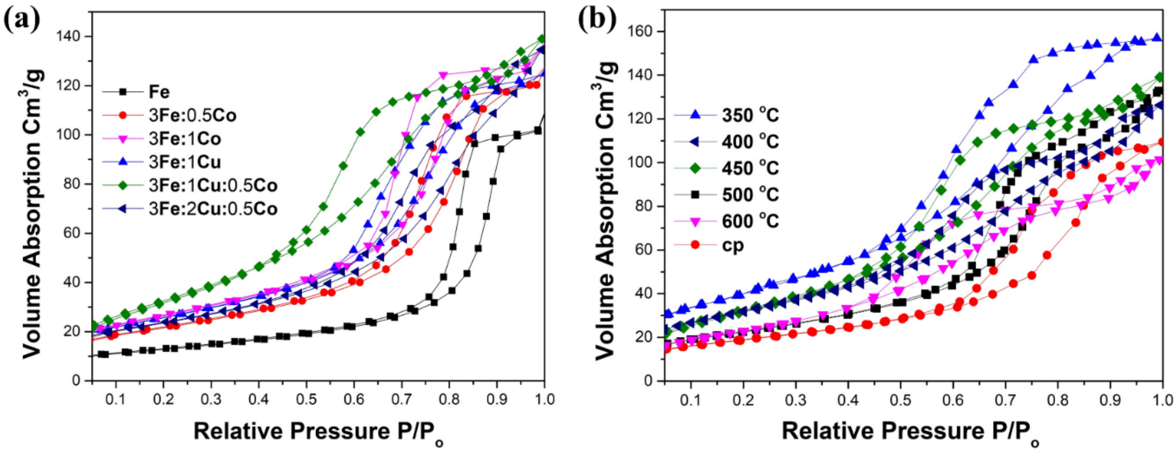

Figure S1. BET Isotherms of (a) different metals, (b) 3Fe:1Cu:0.5Co with different calcination temperature and preparation method

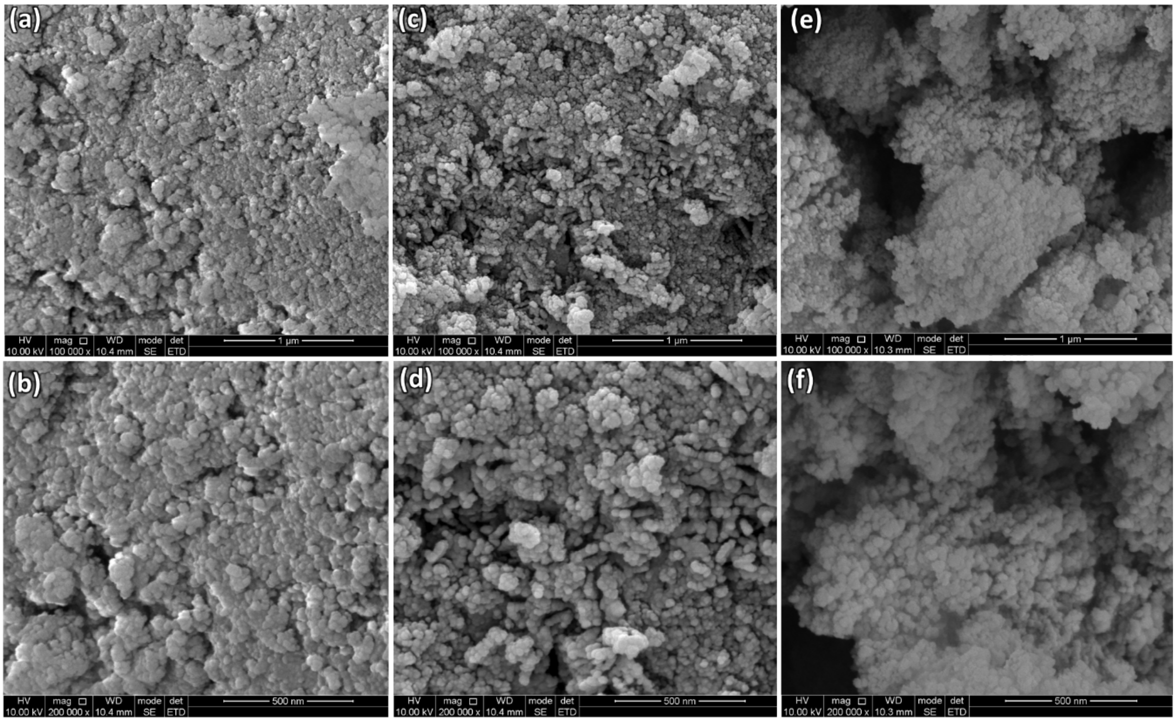

Figure S2. SEM, (a, b) Na-Fe, (c, d) Na-3Fe:0.5Co, (e, f) Na-3Fe:1Cu catalysts

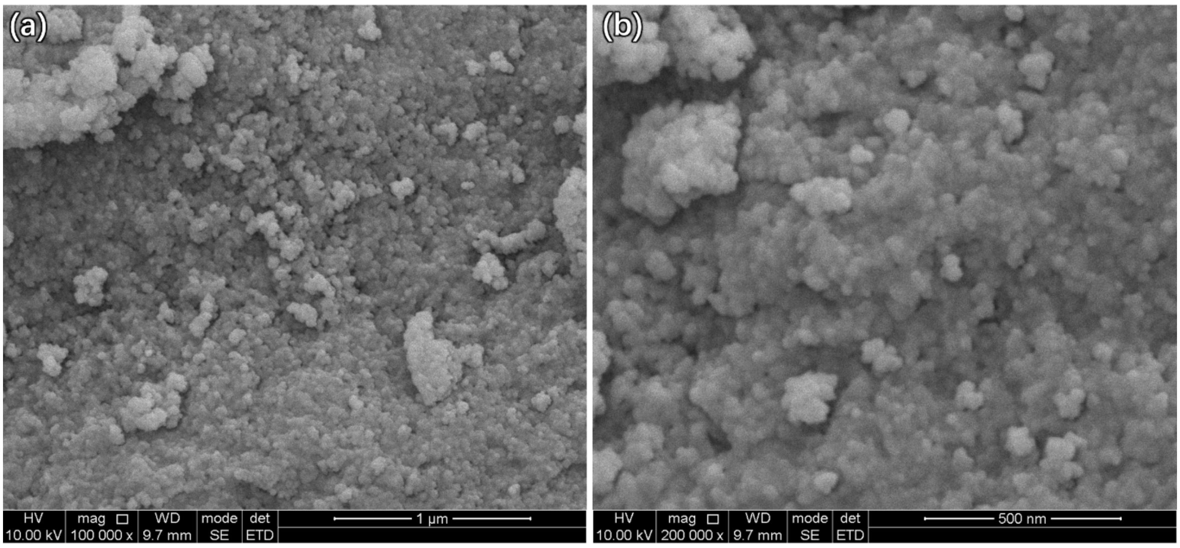

Figure S3. SEM images of Na-3Fe:1Cu:0.5Co^{cp}

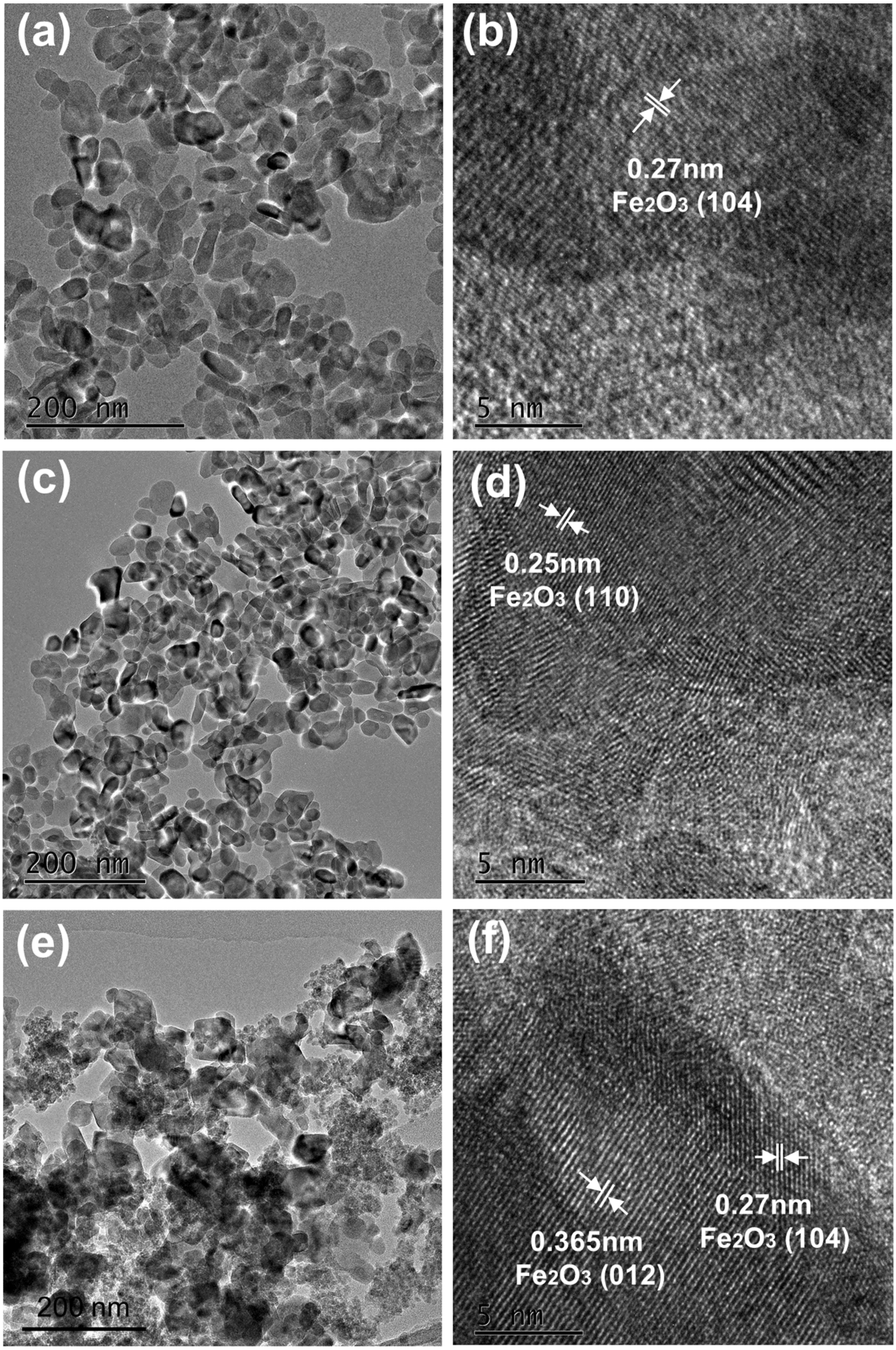

Figure S4. TEM, (e) Na-Fe, (f) Na-3Fe:0.5Co and (g) Na-3Fe:1Cu

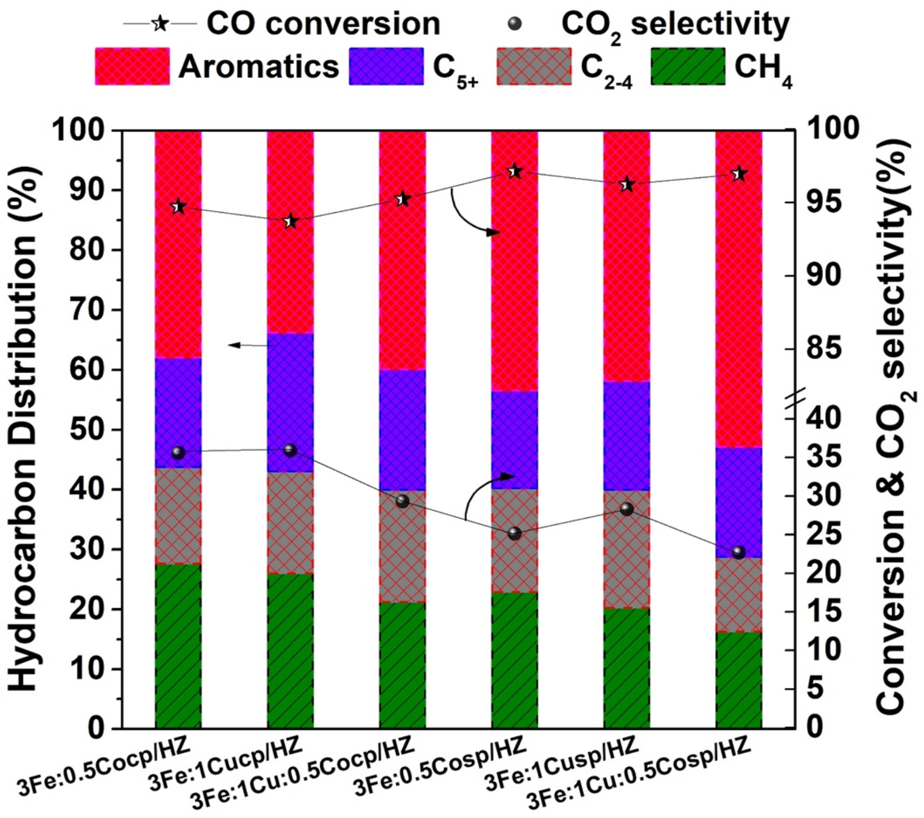

Figure S5. Product distribution of Fe/HZ composite catalyst with co-precipitation and sol-precipitation methods, Reaction conditions: T=340 °C, P=4.0 MPa, GHSV=1500 h^{-1}, H_2/CO=1.5

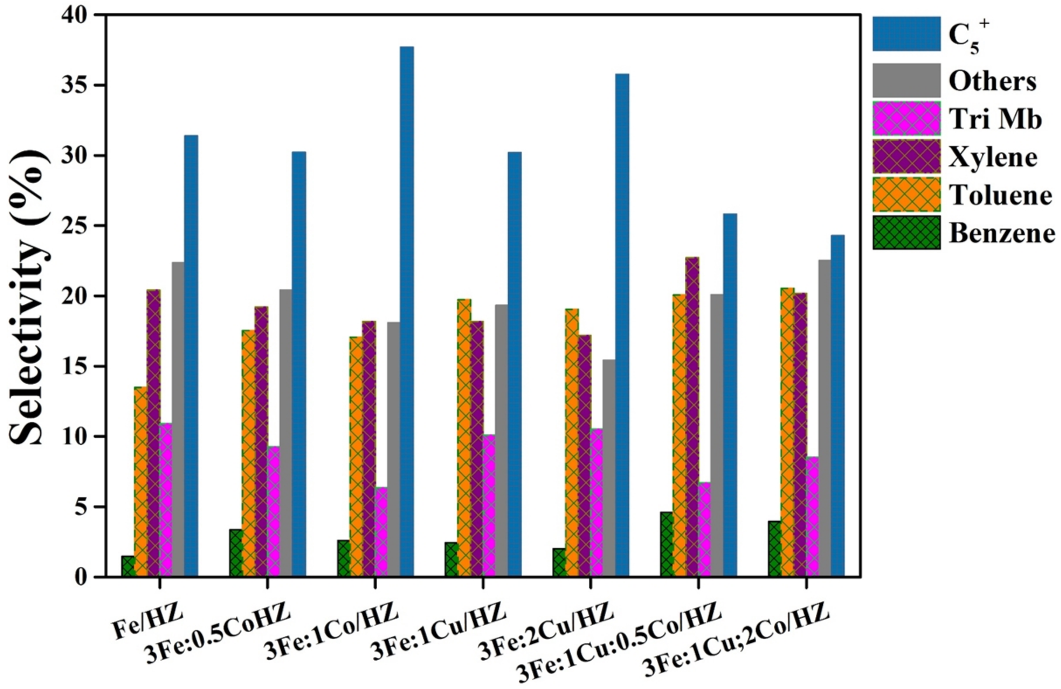

Figure S6. Aromatics distribution of different metal components in Fe/HZ composite catalyst at different calcination temperature, Reaction conditions: T=340 °C, P=4.0 Mpa, GHSV=1500 h^{-1},

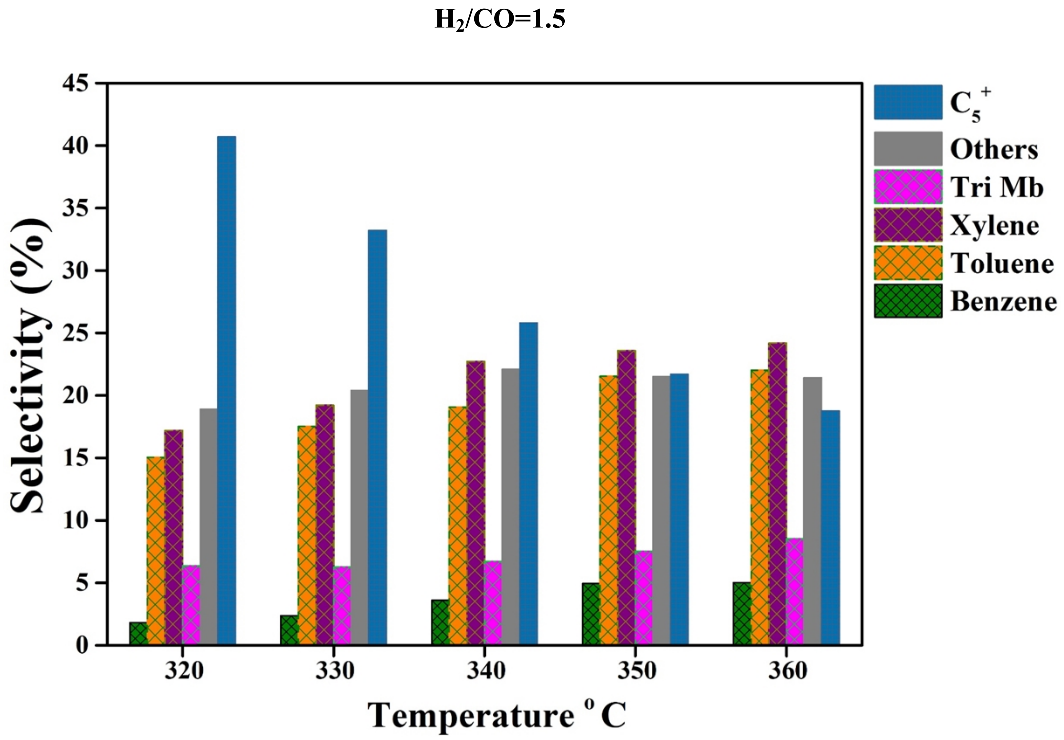

Figure S7 Aromatics distribution of 3Fe:1Cu:0.5Co composite catalyst at different reaction temperature, Reaction conditions: temperature 340 °C, pressure 4 Mpa, space velocity 1500 h^{-1}, $H_2/CO = 1.5$.

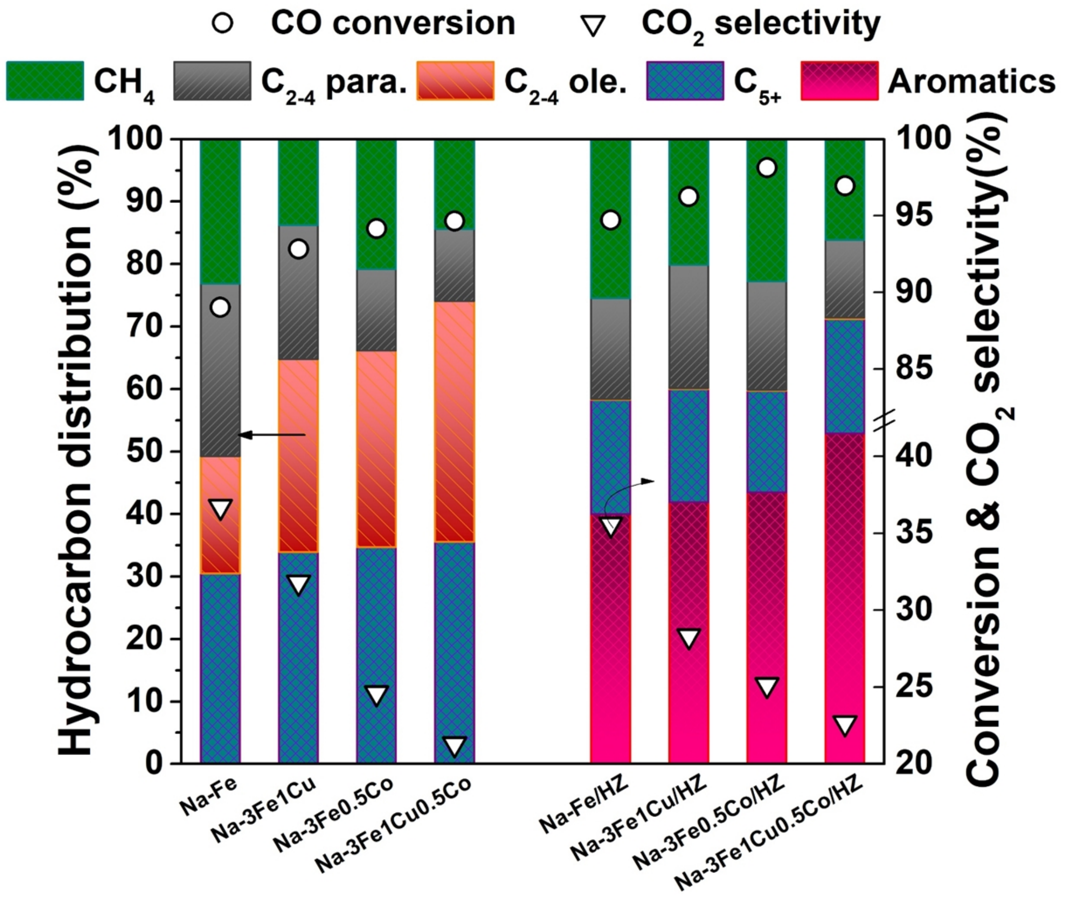

Figure S8. TOS of 3Fe:1Cu:0.5Co/HZ composite catalyst at different calcination temperature, Reaction conditions: temperature 340 ^oC, pressure 4 Mpa, space velocity 1500 h^{-1}, $H_2/CO = 1.5$.

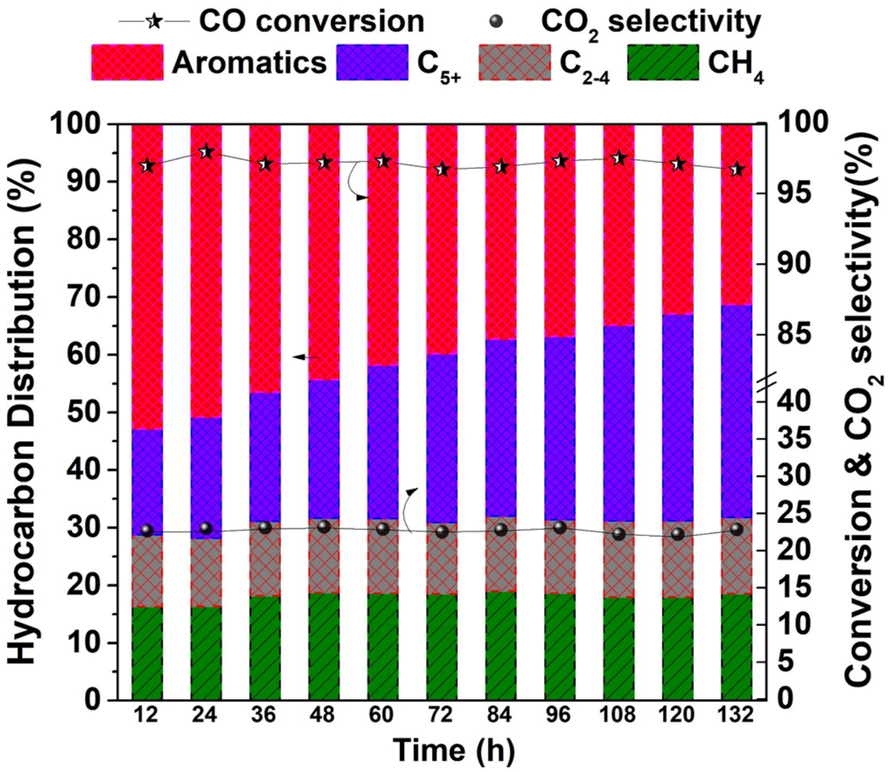

Figure S9. TOS of 3Fe:1Cu:0.5Co/HZ composite catalyst at different calcination temperature, Reaction conditions: temperature 340 ^oC, pressure 4 Mpa, space velocity 1500 h^{-1}, $H_2/CO = 1.5$.

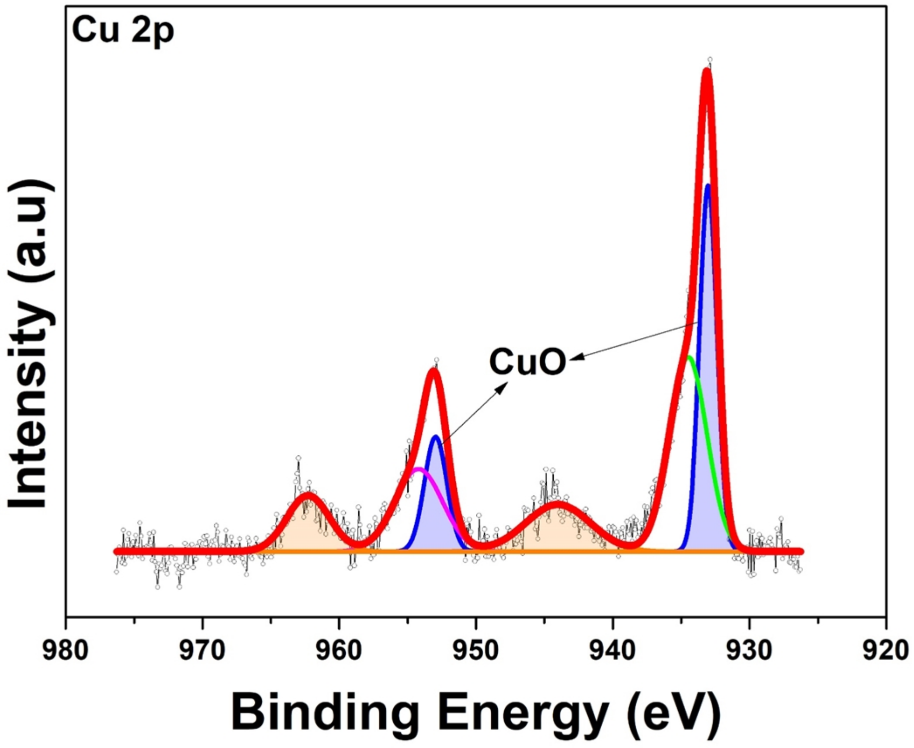

Figure S10. Cu 2p Xps of spent 3Fe1Cu0.5Co catalyst

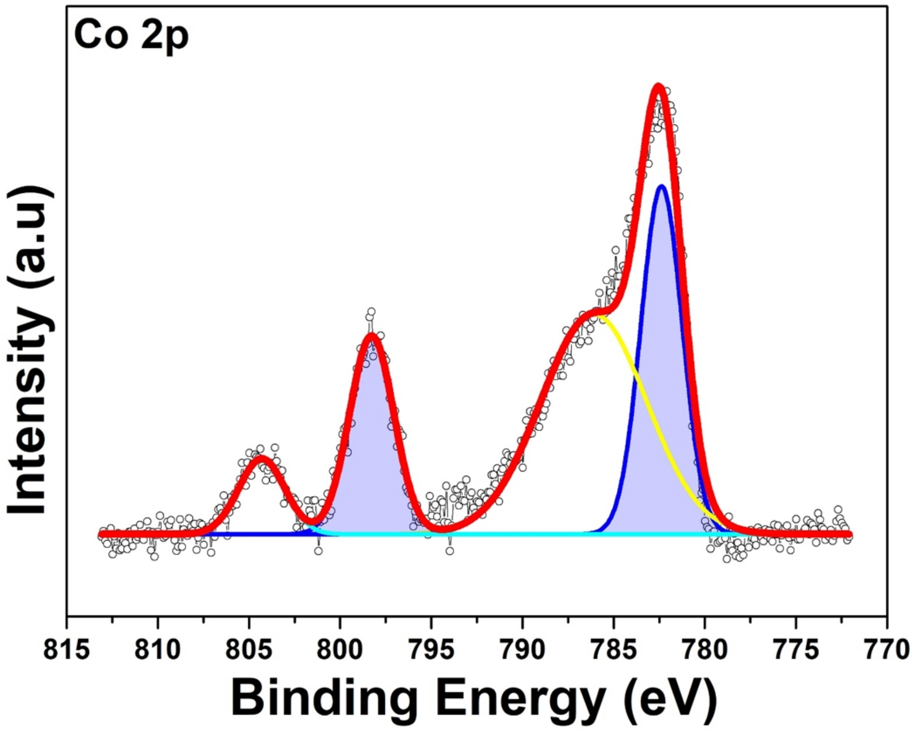

Figure S11. Co 2p Xps of spent 3Fe1Cu0.5Co catalyst

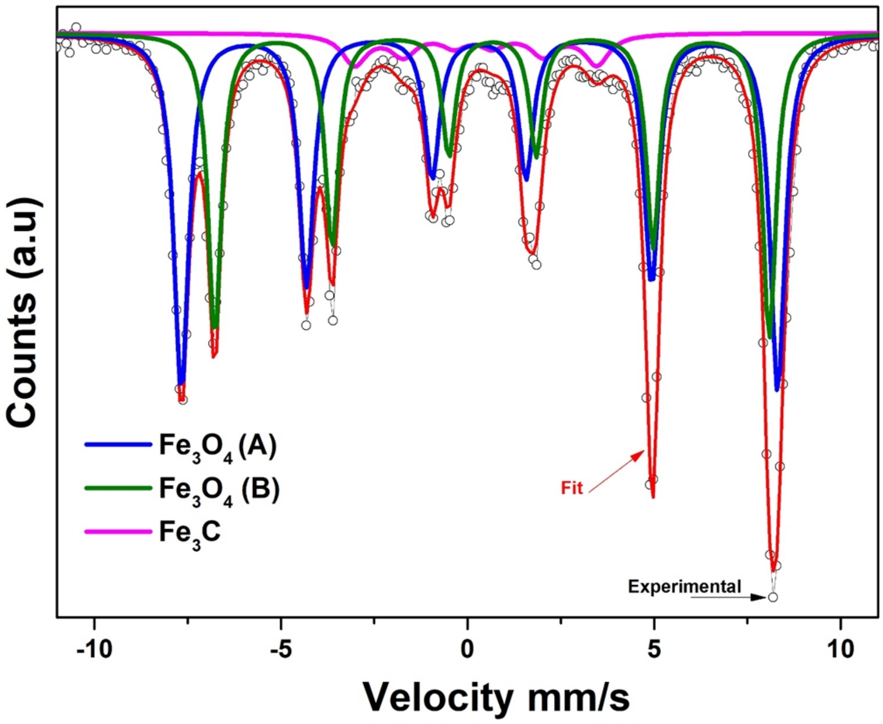

Figure S12. Mossbauer spectra of spent Fe catalyst.

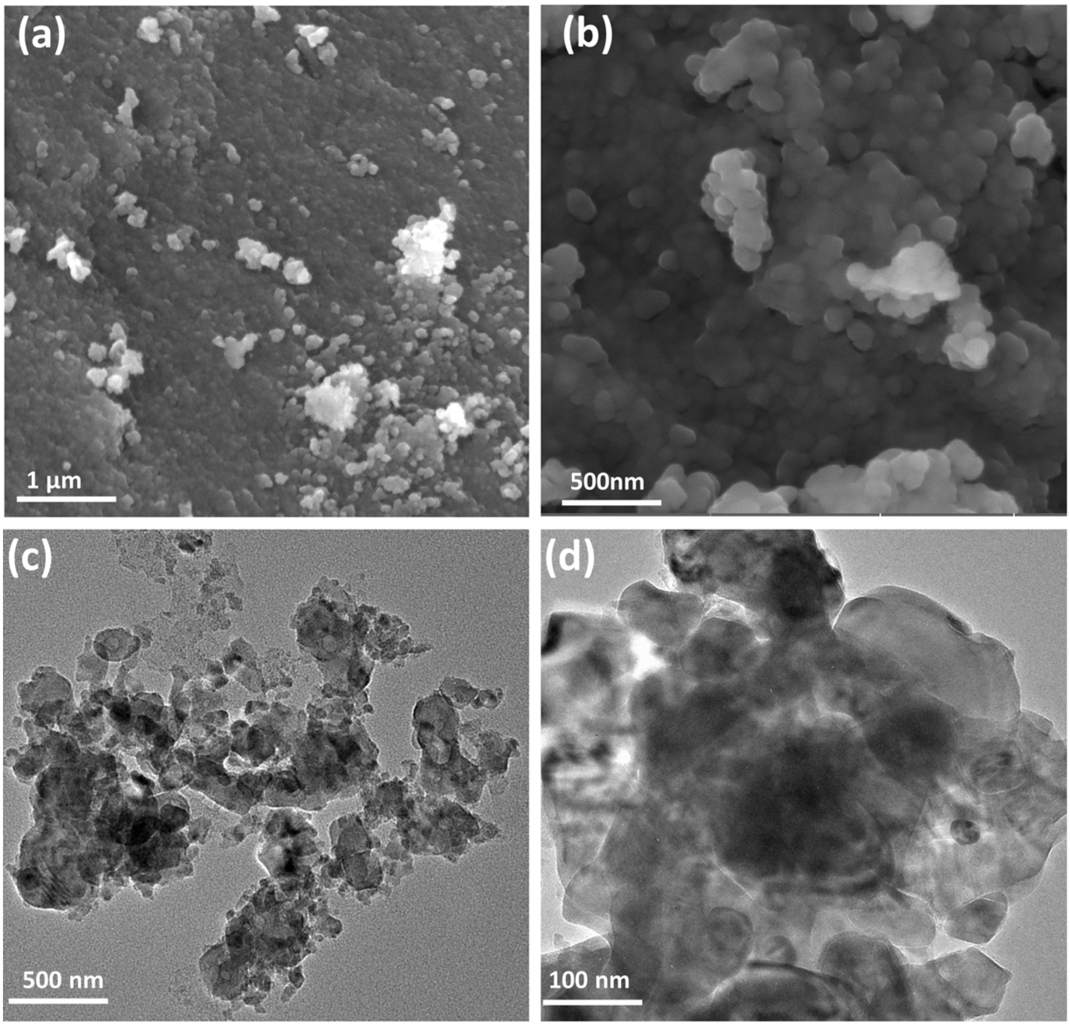

Figure S13. SEM and TEM of spent 3Fe:2Cu:1Co catalyst

Table S1: The chemical compositions of the prepared catalysts obtained by ICP-MS analyses.

Catalyst	Fe (wt %)	Cu (wt %)	Co (wt %)	Na/Fe (wt %)
Na-Fe	91.4	/	/	9.0
Na-3Fe:0.5Co	79.4	/	13.1	/
Na-3Fe:1Co	69.8	/	23.1	/
Na-3Fe:1Cu	70.1	22.8	/	/
Na-3Fe:1Cu:0.5Co	62.1	20.1	10.1	/
Na-3Fe:1Cu:2Co	47.5	14.9	31.3	/
Na-3Fe:2Cu:1Co	47.8	31.5	15.1	/

Where, the sodium amount was maintained as 0.09 with the help of controlled washing times in the centrifugation step, [2, 3].

Table S2 Textural properties of catalyst at different Calcination Temperatures

Sample	S_{BET} (m^2/g)	V_{pore} (cm^3/g)	Pore size(nm)	Crystal size(nm)
Fe	46.10	0.15	13.4	20.19
3Fe:0.5Co	77.25	0.18	9.6	17.8
3Fe:1Co	95.32	0.19	8.06	14.52
3Fe:1Cu	92.61	0.18	8.27	15.22
3Fe:2Cu	72.61	0.15	8.75	15.22
3Fe:1Cu:0.5Co	123.74	0.17	6.56	10.6
3Fe:1Cu:2Co	126.5	0.16	4.95	10.1
3Fe:2Cu:1Co	84.38	0.15	9.01	18.5
3Fe:1Cu:0.5Co ^{cp}	86.63	0.16	7.2	15.5
350 °C	146.53	0.23	4.92	/
400 °C	145.42	0.20	5.04	/
450 °C	137.61	0.18	6.59	9.3
550 °C	86.63	0.16	7.2	15.5
600 °C	81.49	0.15	10.19	19.7
700 °C	68.93	0.15	12.8	21.5

Table S3. Comparative reaction results from literature data

Catalyst	T (°C)	P (bar)	H_2/CO	CO conv. (%)	CO_2 sel. (%)	Hydrocarbon distribution (%)			
						CH_4	C_2-C_4	C_5^+ aliphatics	Aromatics
FeMnLi [4]	320	15	2	85.6	34.6	14.2	36.7	36.1	/
Fe_3O_4@MnO_2 [5]	340	15	2	91.8	37.9	12.0	37.4	45.7	/
Fe/CNF [6]	300	20	2	88.0	42.0	13.0	52.0	18.0	/
Fe-MnK-AC [7]	320	20	1	85.0	48.0	22.7	39.4	29.7	/
FeMnCu [8]	300	20	2	96.9	23.0	20.0	40.1	9.5	/
FeBi/CNT [9]	350	10	1	78.3	47	26.1	35.2	14.1	/
MnCr/HZ [10]	430	40	1	13	45.0	6.7	19.5	2.9	70.9
Fe_3O_4@MnO_2/HZ [11]	320	40	2	64	42	6.1	25.6	20.4	47.9
Fe_3O_4@MnO_2/HZ_{hol} [12]	320	20	1	85	41	5.1	25.4	10.5	59.0
$FeMnKSiO_2$/HZ [13]	300	20	1	63.8	40.2	12.3	19.59	55.2	12.7
KFeMn/HZ [14]	320	25	1	81.1	40.9	12.3	29.7	17.3	40.7
Na-Zn-Fe_5C_2/HZ [15]	350	20	2	88.8	27.5	9.6	26.6	13.2	50.6
ZnCr/HZ [16]	350	40	1	18.3	49	1.5	16.9	27.9	53.6
KFeCo/HZ [17]	310	20	1	98.5	37.9	8.9	35.2	20.8	35.1
3Fe:1Cu:0.5Co/HZ*	340	40	1.5	96.96	22.67	16.31	12.45	18.38	52.85

*Current Work

Table S4. Mössbauer results of reacted Fe, Na-3Fe:0.5Co and Na-3Fe:1Cu:0.5Co catalysts

Figure	Phase	Mössbauer parameters				
		Hhf (kOe)	IS (mm/s)	QS (mm/s)	$\Gamma/2$ (mm/s)	Area (%)
Fe	Fe_3O_4 (A)	494.67	.32	-.01	.24	52.6
	Fe_3O_4 (B)	459.99	.66	.01	.21	39.9
	Fe_3C	200.94	.19	-.06	.4	7.6
Na-3Fe:0.5Co	Fe_3O_4 (A)	491.45	0.31	-0.03	0.15	19.7
	Fe_3O_4 (B)	461.05	0.65	0.02	0.19	37.5
	Fe_5C_2 (I)	216.02	.2	-.12	.18	16.1
	Fe_5C_2 (II)	182.06	.28	.2	.21	12.4
	Fe_5C_2 (III)	112.17	.46	.49	.11	6.5
Na-3Fe:1Cu:0.5Co	Fe_3O_4 (A)	491.2	.32	0	.19	13.8
	Fe_3O_4 (B)	460.65	0.66	0.02	0.19	27.4
	Fe_5C_2 (I)	211.5	.22	-.09	.2	26.6
	Fe_5C_2 (II)	187.62	.22	.03	.21	20.7
	Fe_5C_2 (III)	114.74	.16	.12	.22	6.2

References:

1. M. K. Gnanamani, G. Jacobs, H. H. Hamdeh, W. D. Shafer, F. Liu, S. D. Hopps, G. A. Thomas and B. H. Davis, *ACS Catalysis*, 2016, **6**, 913-927.
2. M. Li, M. A. Nawaz, G. Song, W. Q. Zaman and D. Liu, *Industrial & Engineering Chemistry Research*, 2020, **59**, 9043-9054.
3. X. Cui, P. Gao, S. Li, C. Yang, Z. Liu, H. Wang, L. Zhong and Y. Sun, *ACS Catalysis*, 2019, **9**, 3866-3876.
4. X. Wu, W. Qian, H. Ma, H. Zhang, D. Liu, Q. Sun and W. Ying, *Fuel*, 2019, **257**, 116101.
5. X. Wu, H. Ma, H. Zhang, W. Qian, D. Liu, Q. Sun and W. Ying, *Industrial & Engineering Chemistry Research*, 2019, **58**, 21350-21362.
6. H. M. Torres Galvis, J. H. Bitter, C. B. Khare, M. Ruitenbeek, A. I. Dugulan and K. P. de Jong, *Science*, 2012, **335**, 835.
7. Z. Tian, C. Wang, Z. Si, L. Ma, L. Chen, Q. Liu, Q. Zhang and H. Huang, *Applied Catalysis A: General*, 2017, **541**, 50-59.
8. W. Gong, R.-P. Ye, J. Ding, T. Wang, X. Shi, C. K. Russell, J. Tang, E. G. Eddings, Y. Zhang and M. Fan, *Applied Catalysis B: Environmental*, 2020, **278**, 119302.
9. B. Gu, V. V. Ordomsky, M. Bahri, O. Ersen, P. A. Chernavskii, D. Filimonov and A. Y. Khodakov, *Applied Catalysis B: Environmental*, 2018, **234**, 153-166.
10. D. Miao, Y. Ding, T. Yu, J. Li, X. Pan and X. Bao, *ACS Catalysis*, 2020, **10**, 7389-7397.
11. Y. Xu, J. Liu, J. Wang, G. Ma, J. Lin, Y. Yang, Y. Li, C. Zhang and M. Ding, *ACS Catalysis*, 2019, **9**, 5147-5156.
12. Y. Xu, J. Wang, G. Ma, J. Zhang and M. Ding, *ACS Applied Nano Materials*, 2020, **3**, 2857-2866.
13. Y. Xu, J. Liu, G. Ma, J. Wang, Q. Wang, J. Lin, H. Wang, C. Zhang and M. Ding, *Molecular Catalysis*, 2018, **454**, 104-113.
14. Y. Xu, D. Liu and X. Liu, *Applied Catalysis A: General*, 2018, **552**, 168-183.
15. B. Zhao, P. Zhai, P. Wang, J. Li, T. Li, M. Peng, M. Zhao, G. Hu, Y. Yang, Y.-W. Li, Q. Zhang, W. Fan and D. Ma, *Chem*, 2017, **3**, 323-333.
16. J. Yang, K. Gong, D. Miao, F. Jiao, X. Pan, X. Meng, F. Xiao and X. Bao, *Journal of Energy Chemistry*, 2019, **35**, 44-48.
17. A. Martínez and C. López, *Applied Catalysis A: General*, 2005, **294**, 251-259.